Choi, B. G. & Park, H. S. Superhydrophobic graphene/nafion nanohybrid films with hierarchical roughness. J. Phys. Chem. C. 116, 3207−3211

ARTICLE *in* THE JOURNAL OF PHYSICAL CHEMISTRY C · JANUARY 2012

Impact Factor: 4.77 · DOI: 10.1021/jp207818b

2 AUTHORS:

Bong Gill Choi
Kangwon National University
68 PUBLICATIONS **1,717** CITATIONS
SEE PROFILE

Ho Seok Park
Kyung Hee University
65 PUBLICATIONS **502** CITATIONS
SEE PROFILE

THE JOURNAL OF PHYSICAL CHEMISTRY C

Article

pubs.acs.org/JPCC

Superhydrophobic Graphene/Nafion Nanohybrid Films with Hierarchical Roughness

Bong Gill Choi[†] and Ho Seok Park*[,‡]

[†]Department of Chemistry & Biomolecular Engineering (BK 21), KAIST, 335 Gwahagno, Yuseong-gu, Daejeon 305-701, Republic of Korea

[‡]Department of Chemical Engineering, College of Engineering, Kyung Hee University, Yongin-si 446-701, Republic of Korea

Supporting Information

ABSTRACT: The micro- and macroscopic structures of functional films strongly influence the critical properties, such as superhydrophobicity, which exhibits super water repellency with a water contact angle (CA) larger than 150° for self-cleaning and antimicrobial surfaces. However, it is difficult to achieve the structural hierarchy of two-dimensional graphene for superhydrophobicity. Herein, we report the fabrication of superhydrophobic graphene/Nafion nanohybrid films by controlling the structures with respect to the chemical composition from an interpenetrating networked and compactly interlocked structure (surface area of 9.56 m^2 g^{-1}) to the hierarchical petal-like, porous structure (surface area of 413.46 m^2 g^{-1}). The superhydrophobicity of hybrid thin films with a CA of ~161° was derived from the petal-like structure with hierarchical roughness, where microscale roughness was produced in the lateral direction of hybrid sheets while nanoscopic roughness was created on the edges of hybrid sheets. Furthermore, the wettability and optical and electrical properties of hybrid thin films can be controlled by manipulating the micro- and macroscale structures through the composition-dependent structural changes.

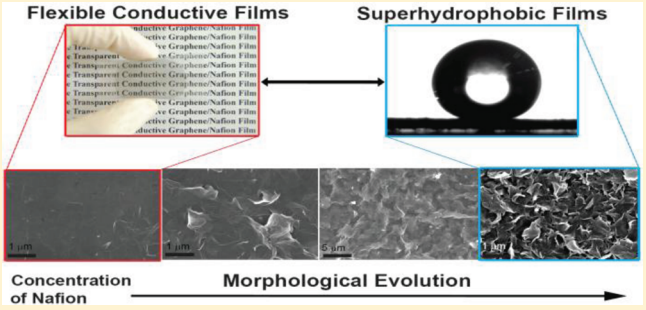

INTRODUCTION

Of pivotal importance in fundamental science and in practical applications is the creation of well-defined structures of materials and objects at multiple scales, owing to strong correlations of structures with physical, chemical, or biological properties.[1] The micro- and macroscopic structures of functional films strongly influence the critical properties, such as superhydrophobicity, which exhibits super water repellency with a water contact angle (CA) larger than 150° for self-cleaning and antimicrobial surfaces.[2] The wetting behavior of thin films is determined by the surface energy of constitutive materials as well as the topological roughness of the surface.[2] In this regard, the superhydrophobic films of energetically unstable materials that cannot be obtained through conventional technology are achieved by the construction of hierarchical, complex nanostructures, showing micro- and nanoscale surface features, such as the lotus or petal effects.[3] Much effort has been devoted to the fabrication of self-cleaning surfaces with the aligned arrays of carbon nanotubes (CNTs), such as forests and pillars.[4] However, these previous studies were limited by the high cost of CNTs and sophisticated processes. Chemically modified graphenes (CMGs) obtained through solution chemistry are highly desirable for the fabrication of a self-cleaning surface because of their processability, large-scale production, and easy chemical functionalization. We fabricated the superhydrophobic films through the controlled assembly of CMG/Nafion (CMGN) hybrids into the complex structures.

Recently, the hybridization of graphene and CMG has received significant attention in the sense that it resolves a major challenge of graphene-based materials, such as the scalable dispersion and poor processability.[5] As a consequence of the synergistic effect of hybridization of multicomponents, furthermore, this technology leads to improving the performance of composite and electronic materials and to rendering new functionalities.[5] For instance, we demonstrated the electronic and ionic conductive CMGN hybrids for electrical and electrochemical applications.[6] However, the structural hierarchy of CMGN hybrids for superhydrophobicity has not yet been explored. Although the superhydrophobic films of graphene-based materials were demonstrated by Lin and Wong et al., they were derived from the reduction of surface energy by means of the functionalization of graphene rather than the topological roughness.[7] Some groups reported the fabrication of superhydrophobic graphene and its composite materials resulting from the rough surface.[8] However, there were no reports about the superhydrophobic thin films of graphene-

Received: August 15, 2011
Revised: November 23, 2011
Published: January 10, 2012

based materials induced by the hierarchically petal-like structure.

Herein, we report the composition-dependent control in the surface and internal structures of CMGN hybrid films for superhydrophobicity. In particular, structural transition of hybrid films occurred from an interpenetrating networked and compactly interlocked structure to the petal-like structure with hierarchical roughness and the porous surface with a high surface area for an application into superhydrophobic films.

EXPERIMENTAL SECTION

Graphite powder (<20 μM), hydrazine solution (35 wt % in water), and Nafion (perfluorinated resin solution, 5 wt % in lower aliphatic alcohol and water mixture) were purchased from Aldrich. 1-Propanol was obtained from Junsei.

Synthesis of Graphene Oxide. In a typical procedure, graphene oxides (GOs) were synthesized from oxidation of natural graphite powder using $KMnO_4$ in a cold solution of H_2SO_4 through a modified Hummers method. To remove remaining metal ions, the resulting mixture of graphite oxides was filtered and washed with 10 wt % aqueous HCl solution (1 L), followed by washing with deionized (DI) water (1 L) to remove the acid. As-obtained graphite oxide powders were diluted with DI water and purified thoroughly by dialysis for 1 week to remove remaining impurities until the filtrated solution was neutral. The powder was then filtered, washed with DI water several times, and dried at 60 °C under vacuum. The exfoliating GOs were prepared in DI water by ultrasonic treatment for 30 min (Fisher Scientific model 500 ultrasonic, 350 W). The complete exfoliation of GOs was confirmed by TEM and AFM images and XRD data, as shown in Figures S1 and S2 (Supporting Information).

Synthesis of CMGN Hybrids. As-prepared GOs (10 mg) were dispersed in 20 mL of DI water and 1-propanol (volume ratio of 50:50). Varying weight ratios of Nafion (2, 10, and 30 wt %) were mixed with 0.5 mg mL^{-1} of GOs in bisolvents. The homogeneous solution of GO and Nafion was prepared by sonication for 60 min and subsequently chemically reducing the mixture by addition of 100 μL of hydrazine solution at 85 °C for 24 h. The resulting mixture was washed with DI water and ethanol several times and purified by dialysis for 1 week.

Characterization. Transmission electron microscopy (TEM) images were collected on an E.M. 912 Ω energy-filtering TEM (EF TEM 120 kV). Scanning electron microscopy (SEM) images were obtained using a field emission scanning electron microscope (FEI Sirion model) equipped with an in-house Schottky emitter in high stability. Atomic force microscopy (AFM) images were recorded in the noncontact mode using a Nanoman Digital Instruments 3100 AFM (VEECO) with an etched silicon aluminum coated tip. The X-ray diffraction (XRD) data were obtained on a Rigaku D/max lllC (3 kW) with a θ/θ goniometer equipped with a Cu Kα radiation generator. The diffraction angle of the diffractograms was in the range of 2θ = 5−40°. FT-IR spectra were collected on a JASCO FT-IR 470 plus. Each spectrum was recorded from 4000 to 650 cm^{-1} using 12 scans at a resolution of 4 cm^{-1}. The X-ray photoelectron spectroscopy (XPS) data were obtained using a Thermo MultiLab 2000 system. An Al Mgα X-ray source at 200 W was used with a pass energy of 20 eV and a 45° takeoff angle under 10^{-7} Torr vacuum in an analysis chamber. The high-resolution scans of C and low-resolution survey scans were analyzed for each sample, taken from at least two separate locations. Sheet resistances of CMGN films were measured by using the standard 4-point probe technique (Loresta-GP, Mitsubishi Chemical). N_2 sorption/desorption data were obtained using a gas sorption analyzer (NOVA 4200 Ver. 7.10). The specific surface area was calculated by the BET equation, and pore size was determined by the BJH model.

RESULTS AND DISCUSSION

The procedures for controlling the structures of CMGN during the fabrication of thin films are illustrated in Figure 1. A modified Hummers method was used to synthesize single layers of fully exfoliated GOs, and the quality was confirmed by TEM, AFM, and XRD (see Figures S1 and S2, Supporting Information). The GOs were readily coated and assembled by the Nafion (a perfluorosulfonated ionomer consisting of a hydrophobic backbone and hydrophilic side chains) through the mutual hydrophobic and hydrophilic interactions between amphiphilic features of GOs and Nafion polymers in an alcoholic solvent, as verified by FT-IR and XPS (see Figures S3 and S4, Supporting Information).[6] After the reduction from GOs to CMG, a homogeneous colloid dispersion of CMGNs still remained. As-obtained CMGNs can be easily dispersed in various solvents, such as water, ethanol, 1-propanol, dimethylformamide, dimethyl sulfoxide, and *N*-methyl-2-pyrrolidone (see Figure S5, Supporting Information). After the reduction step, the hydrophobic interactions between the Nafion backbone and the CMG sheets were strengthened as a result of the restoration of the conjugated structures of CMG and the conformational rearrangement of the amphiphilic Nafion.[6] Despite a few reports on the successful solubilization of CMGs via wet chemistry, CMGs in the absence of Nafion were reaggregated within 1 week, and neither the structural control on a macroscopic scale nor emerging properties, such as superhydrophobicity, have yet been obtained. The dark hybrid solutions impart the high acidity of hydrophilic sulfonic groups tethered to Nafion (ζ potential of −44.2 mV for pure Nafion) for increased solubility, resulting in the high dispersion of CMGNs (~0.5 mg mL^{-1}) and long-term stability over the course of 2 months. Hybrid thin films with the thickness of <1 μm were fabricated by the vacuum filtration (VF) method. The composition-controlled assembly by Nafion enabled us to manipulate the hydrophobicity of the thin film by controlling the surface morphology.

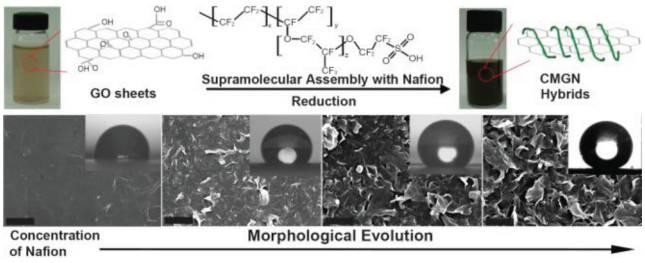

Figure 1. Illustration of a procedure to fabricate CMGNs through supramolecular assembly (top panel) and structural transition of hybrid films with respect to the chemical composition of Nafion, as shown in SEM images (bottom panel). Scale bars are 1 μm. The inset of the bottom panel is the CA photography of CMGN films.

Relevant to the tuning of the structures at the micro- and macroscopic scales are physical and optoelectronic properties of hybrid films that rely on the chemical composition of Nafion.

dx.doi.org/10.1021/jp207818b | J. Phys. Chem. C 2012, 116, 3207−3211

The efficient and uniform coating of individual CMG sheets by Nafion at the molecular level puts them in close proximity, driven by supramolecular interactions,[6] resulting in the approximate thickness of 8 nm of CMGNs, which is attributable to the layer of Nafion (see Figure S6, Supporting Information). Consequently, the inherent electronic properties of CMGs were substantially restored by functionalization with Nafion, despite the high degree of reduction while offering the processability. In an analogue to solvent or surfactant exfoliated CMGs, Nafion-stabilized CMG flakes were folded and their edges wrinkled for minimization of surface energy. The high level of exfoliation and compact packing of CMGNs were capable of generating interlocking structures of the isolated individual sheets (Figure 2), and thus the mechanical integrity

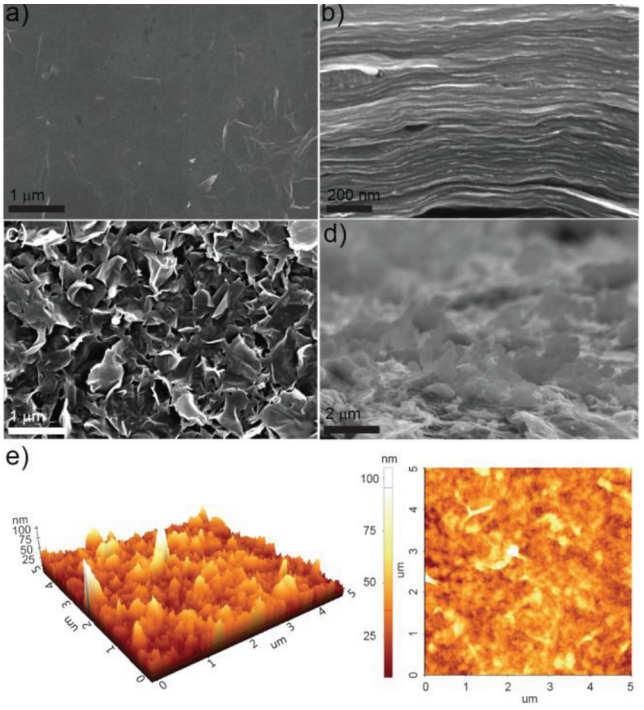

Figure 2. (a) Surface and (b) cross-sectional SEM images of CMGN film at the Nafion loading of 2 wt %. (c) Surface and (d) cross-sectional SEM images of superhydrophobic CMGN film at the Nafion loading of 30 wt %. (e) Non-contact-mode AFM topology and 2D images of CMGN film at the content of Nafion of 30 wt %.

for flexible thin films. Furthermore, the interconnecting networking architectures of the hybrid were constructed by hydrodynamic pressure-driven assembly of randomly arrayed, Nafion-coated CMG sheets in the VF process.

Such structural control of CMGNs is also important for the hydrophobicity of films. As shown in the SEM images of Figure 2, hydrophobic CMGN films at a high loading of Nafion (30 wt %) obtained a rough surface, despite having a similar packed structure of CMGN films. In contrast, the hydrophilic CMGN films at a low loading of Nafion (2 wt %) show a flat and packed structure. The rough surfaces of superhydrophobic CMGN films were confirmed by the analysis of topology using AFM. The surfaces of the hybrid films at a high loading of Nafion exhibited a combination of micro- and nanostructures, and a randomly distributed petal-like microstructure with a thickness of 100 nm. The CAs of the hybrid films can be influenced by various experimental parameters, such as the ratio of CMG to Nafion, flow rate of VF, types of solvents, etc.[9,10] To rule out the effect of other parameters on the hydrophobicity of hybrid films, the amount of Nafion was only varied under identical experimental conditions. The CAs of CMGN films were obtained from the measurement of the contact angles by repeating the water advancing and receding. The CAs were measured at stable stages while receding in order to minimize the difference of advancing and receding contact angles. Compared with the CAs of CMG films, hybrids revealed much higher CAs through simple polymer coating. As the amount of Nafion increased to 30 wt %, the wettability of the thin films decreased due to the reduced surface energy and/or the enhanced roughness of hybrid films. Luo and Sun et al. previously reported that the coating of CNTs by polymers led to superhydrophobic surfaces by reducing the surface energy.[10] In contrast, the superhydrophobicity of thin films could be accomplished by altering the topology through the structural rearrangement during the self-assembly of clay, CNTs, or nanoparticles with polyelectrolytes. Considering the intrinsic hydrophobicity of pristine Nafion (CA = 110°) and the reduction of CA values of hybrids above 30 wt % Nafion,[11] the creation of hierarchical roughness on both nano- and micrometer scales rather than surface energy is more critical for highly water-repellent hybrid films. Microscale roughness was produced in the lateral direction of hybrid sheets by means of the coating effect of Nafion, while nanoscopic roughness was created on the edges of hybrid sheets as a consequence of the perpendicular protrusion of the graphene layers. Moreover, the hybrid films were stable for more than 1 month in a water container owing to their mechanical robustness and superhydrophobicity, whereas CMGs exhibited the destruction of film consolidation.

For a composite system of air pockets and solids, the hydrophobicity of the surface is proportional to the area that the air occupies, following Cassie's Law, as shown in eq 1[10]

$$\cos\theta_c = f_1 \cos\theta - f_2 \quad (1)$$

where $\cos\theta_c$ and $\cos\theta$ denote the CAs of one and multicomponent surfaces and f_1 and f_2 indicate the area fractions of the solid surface and air pockets touched with liquid, respectively ($f_1 + f_2 = 1$). The superhydrophobicity of CMGN films was attributed to the increase in the amount of air trapped on the rough surface, which was derived from the construction of the petal-like structure through the chemical composition dependent structural transition. This finding was supported by the fact that the surface areas and pore volumes of bulk films were dramatically enhanced from 9.56 $m^2\ g^{-1}$ and 0.04 $cm^3\ g^{-1}$ for the compact film to 413.46 $m^2\ g^{-1}$ and 0.45 $cm^3\ g^{-1}$ for the rough film, respectively (see Table S1, Supporting Information). As shown in the bottom panel of Figure 1, the surface morphologies of the hybrids were changed with respect to the amount of Nafion and then their CAs increased from ~97° to ~161°. The structural transition of hybrids from flat to rough surfaces was largely ascribed to the protrusion of the sheet edges toward the surface by means of the Nafion coating, similar to the protrusion of clay functionalized by polyelectrolytes.[12] Benziger et al. reported the switching of the wettability of Nafion film due to surface reorientation.[11] The structural rearrangement of hybrid sheets is related to the complementary interactions between CMG and Nafion. It is worthwhile noting that, in a manner similar to the formation of nanoribbons by poly(*m*-phenylenevinylene-*co*-2,5-dioctoxy-*p*-phenylenevinylene),[13] the favorable interactions

dx.doi.org/10.1021/jp207818b | J. Phys. Chem. C 2012, 116, 3207–3211

of CMG with the hydrophobic backbone of Nafion cause the edges of individual sheets to wrinkle and protrude through structural reorientation. These findings indicate that, as the content of Nafion increases, the respective CMG sheets coated with a hydrophobic backbone of Nafion vertically bulged from the surface to allow for minimal surface energy. In addition, the stability and dispersion of the hybrids in solution result from the reorientation of sulfonic groups in solutions. Therefore, the rough and porous structure of the film surfaces led to the superhydrophobicity by increasing the air trapped in the accessible area. Furthermore, the superhydrophobic CMGN films may be applied into functional, conductive films by optimizing physical properties required for use in self-cleaning electronic devices.

Another important function of CMGN films reflects the fact that the optical and electrical properties of thin films can be controlled by manipulating the chemical composition of hybrids. Figure 3 shows a photo image of a transparent,

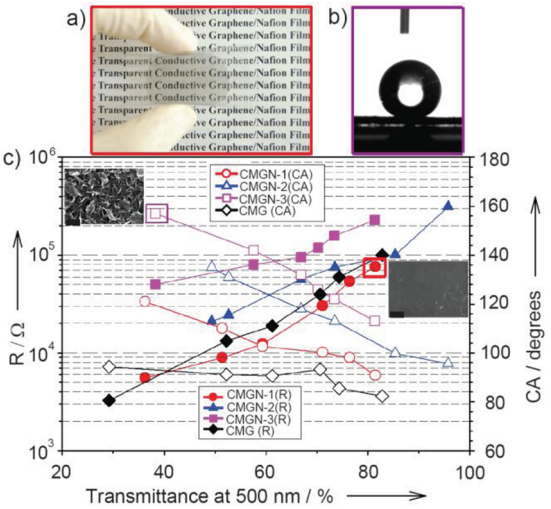

Figure 3. (a) Photography of flexible conductive thin CMGN film. (b) CA photography of superhydrophobic thin CMGN film. (c) CA and sheet resistance (R) versus transmittance of CMGN films. Each CMGN-1, CMGN-2, and CMGN-3 indicate the different Nafion loadings of 2, 10, and 30 wt %. Scale bars in SEM images are 1 μm.

flexible hybrid thin film with a sheet resistance of 80 kΩ cm^{-2} at a transmittance of 80% and a Nafion loading of 2 wt %. At 30 wt % Nafion, the hybrid film exhibited a CA of ~161°. Although the sheet resistance at high transmittance is not sufficient for the application into transparent electrodes, the integration of reasonable flexibility and conductivity with superhydrophobicity can broaden the applicative field of hybrid thin films. Furthermore, the uniform optical and physical properties of thin films can be attributed to the conformal coating of Nafion and the sufficiently good distribution of protruded edges by means of the phase segregation behavior of hybrids and the self-regulating, pressure-driven assembly of the films through the VF process.[14] When the amount of Nafion increased, the sheet resistances and CAs of the hybrid films were enhanced at the constant transmittance of 550 nm up to 30 wt %. In contrast, the hydrophobicity of the single-walled carbon nanotube/Nafion composite was reduced above the Nafion level of ~20 wt %, because of the surface smoothness stemming from the excess Nafion, as previously reported.[10] This discrepancy of optimum Nafion content for superhydrophobicity is related to the geometric differences between 1D and 2D carbon nanomaterials.[10,15] The hybrid films with a lower content of Nafion generated more bicontinuous pathways for the percolated electronic conduction,[6] while decreasing the surface roughness with the formation of a densely compact structure. Therefore, these findings highlight the fact that the wettability, optical and electrical properties, and textural properties of thin films can be controlled by manipulating the micro- and macroscale structures through the composition-dependent structural transition (see Table S1, Supporting Information).

CONCLUSIONS

We demonstrated the preparation of superhydrophobic CMGN hybrid films through the chemical composition dependent structural transition. CMGN hybrid films revealed a petal-like, porous structure with hierarchical roughness, where microscale roughness was produced in the lateral direction of the hybrid sheets while nanoscopic roughness was created on the edges of the hybrid sheets. Moreover, the physical properties of hybrid thin films, such as wettability and optical and electrical properties, were controlled by manipulating the chemical composition. This concept delineated herein envisions the development of functional films based on graphenes and their derivatives as well as the fundamental study of the correlation between the structures and the physical properties of materials on a nanoscale.

ASSOCIATED CONTENT

Supporting Information

TEM and AFM images for GO and CMGN; XRD, FT-IR, and XPS data for GO, GO-Nafion, and CMGN; photograph of CMGN hybrids in various solvents; and textural properties and electrical conductivities of CMG and CMGN films as a function of Nafion loading. This material is available free of charge via the Internet at http://pubs.acs.org.

AUTHOR INFORMATION

Corresponding Author

*E-mail: phs0727@khu.ac.kr.

ACKNOWLEDGMENTS

We acknowledge the financial support by both the National Research Foundation (NRF) funded by the Korean Government (MEST, NRF-2010-C1AAA001-0029018) and the Basic Science Research Program through the National Research Foundation of Korea (NRF) funded by the Ministry of Education, Science and Technology (2011-0007677).

REFERENCES

(1) (a) Min, Y.; Akbulut, M.; Kristiansen, K.; Golan, Y.; Israelachvili, J. *Nat. Mater.* **2008**, *7*, 527. (b) Hu, G.; Ma, D.; Liu, L.; Cheng, M.; Bao, X. *Angew. Chem., Int. Ed.* **2004**, *43*, 3452. (c) Mann, S. *Nat. Mater.* **2009**, *8*, 781.

(2) (a) Li, X. M.; Reinhoudt, D.; Crego-Calama, M. *Chem. Soc. Rev.* **2007**, *36*, 1350. (b) Wang, S.; Jiang, L. *Adv. Mater.* **2007**, *19*, 3423. (c) Feng, X.; Jiang, L. *Adv. Mater.* **2006**, *18*, 3063. (d) Luo, C.; Lei, H. Z.; Wang, L.; Fang, H.; Hu, J.; Fan, C.; Cao, Y.; Wang, J. *Angew. Chem., Int. Ed.* **2010**, *49*, 9145. (e) Hu, W.; Peng, C.; Luo, W.; Lv, M.; Li, X.; Li, D.; Huang, Q.; Fan, C. *ACS Nano* **2010**, *4*, 4317.

(3) Diao, P.; Liu, Z. *Adv. Mater.* **2010**, *22*, 1430.

(4) (a) Pastine, S. J.; Okawa, D.; Kessler, B.; Rolandi, M.; Llorente, M.; Zettl, A.; Fréchet, J. M. J. *J. Am. Chem. Soc.* **2008**, *130*, 4238.

(b) De Volder, M. F. L.; Tawfick, S.; Park, S. J.; Hart, A. J. *ACS Nano* **2011**, *5*, 7310.
(5) Park, S.; Ruoff, R. S. *Nat. Nanotechnol.* **2009**, *4*, 217.
(6) (a) Choi, B. G.; Hong, J.; Park, Y. C.; Jung, D. H.; Hong, W. H.; Hammond, P. T.; Park, H. S. *ACS Nano* **2011**, *5*, 5167. (b) Choi, B. G.; Park, H. S.; Park, T. J.; Yang, M. H.; Kim, J. S.; Jang, S. Y.; Heo, N. S.; Lee, S. Y.; Kong, J.; Hong, W. H. *ACS Nano* **2000**, *4*, 2910.
(7) (a) Lin, Z.; Liu, Y.; Wong, C. *Langmuir* **2010**, *26*, 16110. (b) Lin, Y.; Ehlert, G. J.; Bukowsky, C.; Sodano, H. A. *ACS Appl. Mater. Interfaces* **2011**, *3*, 2200.
(8) (a) Rafiee, J.; Rafiee, M. A.; Yu, Z. Z.; Koratkar, N. *Adv. Mater.* **2010**, *22*, 2151. (b) Zhang, L.; Zha, D.; Du, T.; Mei, S.; Shi, Z.; Jin, Z. *Langmuir* **2011**, *27*, 8943.
(9) (a) Shirtcliffe, N. J.; McHale, G.; Newton, M. I.; Perry, C. C.; Roach, P. *Chem. Commun.* **2005**, 3135. (b) Sun, T.; Liu, H.; Song, W.; Wang, X.; Jiang, L.; Li, L.; Zhu, D. *Angew. Chem., Int. Ed.* **2004**, *43*, 4663.
(10) Luo, C.; Zuo, X.; Wang, L.; Wang, E.; Song, S.; Wang, J.; Wang, J.; Fan, C.; Cao, Y. *Nano Lett.* **2008**, *8*, 4454.
(11) Goswami, S.; Klaus, S.; Benziger, J. *Langmuir* **2008**, *24*, 8627.
(12) Jisr, R. M.; Rmaile, H. H.; Schlenoff, J. B. *Angew. Chem., Int. Ed.* **2005**, *44*, 782.
(13) Li, X.; Wang, X.; Zhang, L.; Lee, S.; Dai, H. *Science* **2008**, *319*, 1229.
(14) (a) Zhang, J.; Gao, L.; Sun, J.; Liu, Y.; Wang, Y.; Wang, J.; Kajiura, H.; Li, Y.; Noda, K. *J. Phys. Chem. C* **2008**, *112*, 16370. (b) Dikin, D. A.; Stankovich, S.; Zimney, E. J.; Piner, R. D.; Dommett, G. H. B.; Evmenenko, G.; Nguyen, S. T.; Ruoff, R. S. *Nature* **2007**, *448*, 457.
(15) Zhang, L. L.; Zhao, X. S. *Chem. Soc. Rev.* **2009**, *38*, 2520.